THE MICROSTRUCTURE AND MICROCHEMISTRY OF AMOEBOID OLIVINE AGGREGATES FROM THE ALHA 77307 CO3.0 CARBONACEOUS CHONDRITE: CONSTRAINTS ON FORMATION AND THERMAL HISTORIES. Jangmi Han[1] and Adrian J. Brearley[1], [1]Department of Earth and Planetary Sciences, MSC03-2040, 1University of New Mexico, Albuquerque, NM 87131, USA. (E-mail: jmhan@unm.edu; brearley@unm.edu).

Introduction: Amoeboid olivine aggregates (AOAs) are widely interpreted as the primary products of gas-solid condensation from the cooling solar nebula, which subsequently experienced high-temperature annealing and, in some cases, a small degree of melting. Forsteritic olivine is the major phase in AOAs, occurring with lesser, variable amounts of refractory Ca-Al-rich phases such as Al-Ti-bearing pyroxene, ±anorthite, and ±spinel. Rarely, melilite and perovskite are present [e.g., 1,2].

Recently, our preliminary TEM studies have suggested that refractory Ca-Al-rich phases from AOAs show clear evidence of reactions between condensed solids and the nebular gas phase [3]. Here, in a continuing effort, we present new microstructural and microchemical observations obtained by TEM on olivine and refractory Ca-Al-rich phases in AOAs from the primitive CO3.0 chondrite, ALHA 77307 [4], and discuss their implications for the formation and thermal histories of the AOAs.

Methods: About 80 AOAs from a thin section of ALHA 77307 (CO3.0) were identified by elemental X-ray mapping and BSE imaging on a FEI Quanta 3D FEG-SEM/FIB operating at 30kV. Four representative AOAs (#4-7) were selected for further detailed TEM studies. We prepared five sections from the AOAs using FIB techniques; three sections from AOAs #4, 5, and 6 were cut from a region where refractory components are present and two sections from AOA #7 were sampled from olivine grains. The FIB sections were studied using bright-field and scanning transmission electron imaging, electron diffraction, and analytical electron microscopy (AEM) on a JEOL 2010F FASTEM FEG scanning TEM operating at 200kV to characterize their microstructures and microchemistry.

Results: The four AOAs we investigated in this study are porous and irregular in shape. They consist predominantly of forsteritic olivine grains with minor refractory Ca-Al-rich phases such as fine-grained spinel, anorthite, and diopside. No melilite or perovskite were present in any of the AOAs studied. The refractory phases occur as interstitial phases between olivine grains or as large, dense CAI-like objects. All AOAs contain Fe-Ni metal and oxide grains, the latter probably being terrestrial weathering products.

AOAs #4 and 6 are less than 150μm in size and texturally very similar. The refractory phases in these AOAs have a ragged, irregular appearance (Fig. 1a). AOA #5, ~130μm in size, contains areas (up to ~30μm in size) consisting of fine-grained intergrowths of spinel, anorthite, and diopside. The inclusions are surrounded by relatively compact olivine grains (Fig.1b). Chromium Kα X-ray maps of three AOAs (#4-6) obtained by FEGSEM, using an SDD EDS detector, show that Cr is preferentially concentrated in the refractory components. In AOA #7, the refractory components occur mostly as elongated masses, rather than as interstitial phases between olivine grains. AOA #7 is locally porous, but some parts of the AOA are compact with a low porosity.

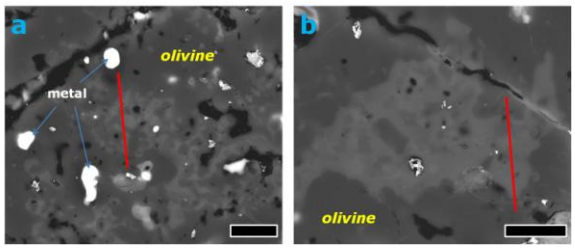

Figure 1. BSE images of (a) AOA #4 and (b) AOA #5. Refractory components occur (a) as interstitial phases or (b) as CAI-like inclusions. Red bars indicate the positions of FIB sections. Black scale bars are 10μm in length.

TEM observations. Three FIB sections were prepared from refractory components in AOAs #4, 5, and 6. Spinel, diopside, and olivine commonly occur in all three FIB sections, and anorthite is present in the FIB sections from AOAs #4 and 6. Iron-nickel metal grains are found in AOA #4 and 5. Two FIB sections sampled from AOA #7 consist of dense aggregates of ~1-5μm-sized olivine grains. All sections contain pores of various sizes and shapes. Grain boundaries between all these refractory phases are very embayed and curved, indicating a reaction relationship between phases. Paradoxically, triple junctions between olivine grains and between olivine and refractory phases from all AOAs are common which suggests that the AOAs have been annealed after agglomeration. Most grains are free of dislocations or defects, but rarely diopside grains have low densities of dislocations in localized regions.

AEM analyses show that in all FIB sections olivine is very close to pure forsterite with ≤0.3 wt.% FeO and plagioclase is nearly pure anorthite. Both phases have very uniform compositions in all the AOAs. In contrast, there are large variations in the chemical compositions of spinel and pyroxene. The compositional data for spinels show they have constant MgO contents, but variable Al_2O_3 (54-74wt.%) and Cr_2O_3 (1-16wt.%)

contents, with Al_2O_3 content inversely correlated with Cr_2O_3 content, as would be expected, due to the coupled substitution between Cr^{3+} and Al^{3+}. Individual spinel grains are unzoned, but variations in Al_2O_3 and Cr_2O_3 contents are observed from one grain to another both within a single FIB section and from one section to another. Pyroxene compositions in this study exhibit the same remarkable variations in chemical compositions within single grains and between grains, as we have reported previously [3]. The total range of Al_2O_3 contents in pyroxene from the AOAs studied is 3 to 32wt.%, and TiO_2 contents from 0 to 18wt.%. Pyroxene from AOA #6 is notable, because it contains two distinct compositional ranges; pyroxene grains in contact with anorthite have very low, constant TiO_2 contents, ≤0.5wt.%, with 2-13wt.% Al_2O_3, but pyroxene grains in contact with spinel have a much wider range and higher contents of Al_2O_3 and TiO_2 (4-32wt.% Al_2O_3; 1-18wt.% TiO_2). In AOA #5, pyroxene grains in contact with spinel have higher Al_2O_3 contents than pyroxene grains which are not associated with spinel, at least within the 2D slice represented by the FIB section. Some pyroxene grains from AOA #6 have higher TiO_2 contents compared to those from AOAs #4 and 5 with similar Al_2O_3 contents (Fig. 2).

One Fe-Ni metal grain was found in each of the FIB sections from AOA #4 and 5. Both grains are kamacite; $Fe_{97}Ni_3$ in AOA #4 and $Fe_{91}Ni_9$ in AOA #5. In AOA #4, schreibersite ($Fe_{30}Ni_{46}P_{25}$) occurs at the edge of the kamacite grain, whereas in AOA #5 a Cr-bearing Fe metal grain ($Fe_{96}Cr_4$) is associated with the kamacite.

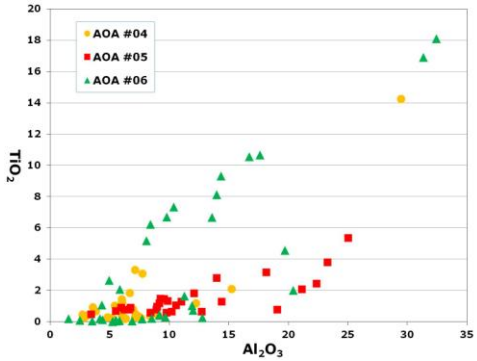

Figure 2. A plot of TiO_2 versus Al_2O_3 (wt.%) for pyroxene from AOAs #4, 5, and 6 (AEM EDS data).

Discussion: The textural and compositional relationships between pyroxene and spinel in these AOAs are strongly indicative of a reaction relationship between the minerals, consistent with our previous observations from other AOAs [3]. However, these relationships are complex and not identical in each AOA, indicating that individual AOAs may have experienced somewhat different thermal histories. Pyroxenes associated with spinel in AOA#4 and #5 show systematically higher Al_2O_3 contents with only modest increases in TiO_2 contents. We attribute these trends in the pyroxene chemical composition to a direct reaction of spinel with a gas phase to form Al-rich diopside. This reaction appears not to involve melilite due to the lack of melilite in any of the FIB sections studied. The compositional trends in pyroxene in AOA #6 are quite distinct, with strong, correlated increases in TiO_2 content as Al_2O_3 content increases. In general, the highest Al_2O_3 and TiO_2 contents occur closest to the spinel grains (Fig. 2). In this case, reaction of a gas phase with spinel to form pyroxene must have occurred under conditions where fractional condensation of Ti had not occurred. However, rather than forming discrete Ti-rich phases such as perovskite or Ti-oxides [3], Ti was concentrated in the pyroxene. Preservation of this extreme chemical heterogeneity in pyroxene over very short distances suggests relatively fast cooling following the gas-solid reactions [3].

No previous studies of AOAs have described elevated Cr contents in spinel, such as those found in this study. Spinels in AOAs typically have Cr_2O_3 contents <0.5wt% [1]. The only viable mechanism for enriching Cr in spinel grains is by progressive resorbtion of the spinel during reaction with a gas phase. In this scenario, Cr is preferential retained and concentrated in the unreacted, residual spinel.

Conclusions: Our microstructural and microchemical data for the four AOAs show a high degree of textural and compositional disequilibrium among the refractory CAI-like phases. In particular, we observe strong evidence in all the AOAs of disequilibrium reactions with a nebular gas that resulted in the progressive resorbtion of spinel to form Al-Ti-rich diopside. Contrary to previous suggestions, we find no evidence that these reactions involved melilite. Our data also suggest that the conditions under which these reactions occurred were not identical for all AOAs, as recorded in differences in pyroxene chemistry, notably their Ti contents. In contrast to the refractory phases, the olivines in all the AOAs display strong textural evidence of equilibrium. These data demonstrate that AOAs have experienced very complex formational and thermal histories, including high-temperature condensation, reaction of solids with the nebular gas, and annealing, under highly dynamic conditions [3].

Acknowledgements: This work was funded by NASA grant NNX11AK51G to A. J. Brearley (PI).

References: [1] Krot A. N. et al. (2004) *Chemie der Erde, 64,* 185-239. [2] Grossman L. and Steele I. M. (1976) *Geochim. Cosmochim. Acta, 40,* 149-155. [3] Han J. and Brearley A. J. (2011) *Workshop on Formation of the First Solids in the Solar System*, Abstract #9084. [4] Grossman J. N. and Brearley A. J. (2005) *Meteoritics & Planet. Sci., 40,* 87-122. [5] Komatsu M. et al. (2001) *Meteoritics & Planet. Sci., 36,* 629-641.